Numerical Study on the Smoke Flow Characterization and Phenomenon of Plug-Holing under Lateral Smoke Exhaust in Tunnel Fire

J. Yang, X. Pan[†], Z. Wang, M. Hua and J. Jiang

College of Safety and Engineering, Nanjing Tech University, Nanjing, China
Institute of Fire Science and Engineering, Nanjing Tech University, Nanjing, China
Jiangsu Key Laboratory of Urban and Industrial Safety, Nanjing, China

†*Corresponding Author Email: xuhaipan@njtech.edu.cn*

ABSTRACT

Although the lateral smoke extraction system had been adopted in the tunnel and subway, the research on the efficiency of the lateral smoke exhaust system is still lacking. A set of numerical simulations were conducted using Fire Dynamic Simulator (FDS) to analyze the plug-holing phenomenon under lateral smoke extraction system in the tunnel fire. Taking an actual lateral smoke exhaust system in a road tunnel as the prototype, a series of fire cases were simulated, wherein the heat release rate (HRR) of the fire source and mechanical exhaust rate, in particular, varied. The smoke flow characteristic in the lateral exhaust system is analyzed and phenomenon of plug-holing was observed. The temperature and smoke layer near the lateral smoke vent are analyzed, and results show that the phenomenon of plug-holing will decrease the lateral smoke exhaust system performance. The exhausting efficiency would not change significantly as the exhaust rate increasing. The critical Froude number we calculated to determine the phenomenon of plug-holing under lateral smoke exhaust in tunnel fire is 0.48, meanwhile, a saturated Froude number 1.95 was introduced by taking account of a better exhaust efficiency.

Keywords: CFD; Plug-holing; Mechanical smoke exhaust; Froude number.

NOMENCLATURE

A	smoke vent area	Pr	*Prandtl* number
c_p	specific heat at constant pressure	Q	fire power
Cs	smagorinsky constant (LES)	Sc	*Schmidt* number
d	depth of the smoke layer	T_0	environmental temperature
D^*	characteristic length of fire source	ΔT	temperature difference
Fr	Froude number	T_{amb}	temperature of ambient air
g	acceleration of gravity	T_{int}	temperature at the interface
Ls	physical model size of simulation		
Le	physical model size of experiment	ρ_0	environmental air density
$\dot{m}$	mass flow		

1. INTRODUCTION

With the improvement of tunnel construction systems, the tunnels are becoming longer and more complex, so the possibility and risks of fire accidents increases (Steckler *et al.* 1984; Morgan 1990; Ciambelli *et al.* 2011; Carvel Ricky 2015). Because the lack of the routes for people's evacuation and fire services, fire happened in tunnels could lead to severe consequences (Guo *et al.* 2007; Wen *et al.*

2007; Chow *et al.* 2015). In the past years, some serious fires have taken place in the different tunnels around the world. For example, a truck caught fire in Mont Blanc Road Tunnel because of the flour and margarine in 1999, which burned for 53 hours and caused 38 people died at least (Vuilleumier, *et al.* 2002). A train caught fire in Kitzsteinhorn Tunnel in Austria on November 2000, because of hydraulic oil leak age to electrical heater, and caused 155 people died (Schuper 2001). An arson fire occurred in

Daegu Subway, Korea, 198 people died and 151 people injured on February, 2003 (Lee and HUR 2012). Statistics on fire accidents showed that thermal damage and smoke inhalation are the primary causes of death for victims in tunnel fires (Lougheed and Hadjisophocleous 2001; Richard G. Gann 2004). In order to control and remove smoke inside tunnels quickly, mechanical extraction systems should be adopted in tunnel properly.

The efficiency of the mechanical extraction systems had been investigated in the past few years. Heselden *et al.* (1974) conducted both large and small-scale experiments on fires in building, and pointed out that a large extraction rate at a given point will draw up fresh air into the extraction duct and will markedly reduce the actual amount of smoky gases removed. He also claimed that the maximum extraction rate before air is drawn up into the extraction duct depends on the layer depth and temperature, and a simple expression has been derived. Morgan *et al.* (1990) claimed that a Froude number for vents near the centre of a smoke reservoir is 1.5 and the Froude number for vents near the side walls is 1.1. A lot of experiments were carried out in a large-scale physical model by Lougheed *et al.* (2002) and the results indicated that plug-holing equation provided by Hinkley can be applied in mechanical exhaust system. Viot *et al.* (2001) studied the critical condition associated with the plug-holing phenomenon in experiments and numerical simulations and concluded that it is better to use several small vent than a big vent in order to reduce the depth of plug-holing and to extract the smoke more efficiently. Hu *et al.* (2006) experimentally studied the efficiency of mechanical extraction system in a full-scale atrium and claimed that when the smoke layer is thin enough and smoke exhausting rate is large enough, the fresh air from below the interface were entrained into the smoke layer and had a large proportion of the smoke exhausting volume, which caused the efficiency of the mechanical extraction system decreased obviously. Vauquelin *et al.* (2008) noticed the phenomenon of plug-holing in a small-scale tunnel and found that the smoke exhaust efficiency had obviously decreased due to the fresh air being inhaled into the smoke vent. Ji *et al.* (2013) carried out a series of numerical simulations to study the Froude number used in tunnel and found that the critical Froude number 1.5 isn't suitable for tunnel fire, a Froude number of 2.1 is applicable for roof-venting tunnel.

However, former studies are focusing on the smoke vent mounted in the ceiling, severely former researches had been performed to study the plug-holing in the lateral smoke extraction system. The phenomenon of plug-holing and the relationship between the exhausting rate and the smoke layer are rarely discussed in the literatures. Actually, the prediction of occurrence of plug-holing in lateral smoke exhaust system is significant, due to exhausting efficiency for smoke control. In this paper, numerical simulations are conducted to find out the Froude number in tunnel fire with lateral extraction system. Different heat release rates (HRRs) of fire are engaged and a new Froude number is proposed for the fire safety managements.

2. CFD NUMERICAL MODELLING

2.1 An Introduction to Fire Dynamics Simulation

FDS is a fire dynamic software developed by the National Institute of Standards and Technology (NIST). FDS solves numerically a set of the Navier-Stokes equations suitable for low-speed (Ma < 0.3), thermally-driven flow focusing on the smoke and heat transport from fires. The Direct Numerical Simulation (DNS) or the Large Eddy Simulation (LES) can be used for turbulence calculations within FDS (Kevin McGrattan *et al.* 2015). DNS solves Navier-Stokes equations numerically without any turbulence model which can be extremely time-consuming. LES solves Navier-Stokes equations numerically by ignoring the smallest length scales via a low-pass filtering model, which is widely used in fire-induced smoke flow behaviour. The version of FDS adopted for simulation is 6.5.1 and LES is selected in this study for turbulence calculations (Kevin McGrattan *et al.* 2015). The controlling equations for LES in FDS are shown as follows:

The conservation of mass

$$\frac{\partial \rho}{\partial t} + \nabla \cdot \rho u = \dot{m}_b''' \tag{1}$$

The conservation of momentum

$$\frac{\partial}{\partial t}(\rho u) + \nabla \cdot \rho uu + \nabla p = \rho g + f + \nabla \cdot \tau_{ij} \tag{2}$$

The conservation of energy

$$\frac{\partial}{\partial t}(\rho u) + \nabla \cdot \rho hu = \frac{Dp}{Dt} + \dot{q}''' - \nabla \cdot \dot{q}'' + \phi \tag{3}$$

In FDS, the SGS momentum and scalar flux terms is calculated by the gradient diffusion in the turbulence model. A model for the turbulent transport coefficient is required: the turbulent viscosity or the turbulent diffusivity. Schmidt number (for mass diffusivity) or Prandtl number (for thermal diffusivity) is adopted to obtain the turbulent diffusivity, and viscosity is the most important transport coefficient should be concerned (Kevin McGrattan *et al.* 2015). By default, FDS uses a variation of Deardorff's model:

$$\mu_t = \rho C_v \Delta \sqrt{k_{sgs}} \tag{4}$$

$$k_{sgs} = \frac{1}{2}\left(\left(\overline{u} - \hat{\overline{u}}\right)^2 + \left(\overline{v} - \hat{\overline{v}}\right)^2 + \left(\overline{w} - \hat{\overline{w}}\right)^2\right) \tag{5}$$

$\overline{u}$ is the average value of *u* at the grid cell centre and $\hat{\overline{u}}$ is a weighted average of *u* over the adjacent cells (Kevin McGrattan *et al.* 2015). The value C_v is set to be 0.1 in this paper according to the former researches. In the simulation, the parameters related to the turbulent viscosity are the thermal conductivity and mass diffusivity, given by

$$k_{SGS} = \frac{\mu_{SGS} C_p}{Pr} ; \quad (\rho D)_{LES} = \frac{\mu_{SGS}}{Sc} \tag{6}$$

Table 1 Computing details of FDS simulations

Test no.	Grid number in axis			Grid size	Total number of grids	Time consuming(h)
	x	y	z	δx(m)		
1	100	1020	72	0.1	7711200	119.84h
2	70	680	48	0.15	2284800	20.53h
3	50	510	36	0.20	954720	8.2h
4	34	340	24	0.30	285600	2.22h
5	25	255	18	0.40	119340	0.36h

Computational domain: 10.5m(x) x 102m(y) x 7.2m (z)

NIST provided many model verification and experimental validation since the first version of FDS had been released in 2000. According to those validation models, the turbulent Prandtl number **Pr** and the turbulent Schmidit number **Sc** are set for this paper as 0.2 and 0.5, respectively (Chow *et al.* 2008). Also, for stability conditions, The Courant-Friedrichs-Lewy (CFL) constraint given by

$$\mathbf{CFL} = \mathbf{\delta t} \cdot \frac{\|u\|}{\delta x} \approx 1 \qquad (7)$$

$$\frac{\|u\|}{\delta x} = \mathbf{max}(\frac{|u|}{\delta x}, \frac{|v|}{\delta y}, \frac{|w|}{\delta z}) \qquad (8)$$

needs to be fulfilled. The CFL constraint places a restriction on the time step due to the advection velocity. For LES, this constraint has an additional advantage of keeping the implicit temporal and spatial consistent with each other to maintain stability (Kevin McGrattan *et al.* 2015).

In the LES simulation, the method to determine the convective heat transfer coefficient (h) is the natural and forced convection correlations. The thermal radiation commonly referred to be the radiation fraction is the most important radiation parameter in LES, and the radiation fraction is set to be 0.35. The Eddy Dissipation model is adopted and the Smagorinsky Constant is specified as 0.2 in this paper (Kevin McGrattan *et al.* 2015).

2.2 Validation and Grid Sensitivity

A mesh sensitivity study is an important measure to ensure a reasonable simulated results (Tilley *et al.* 2011). In this paper, the mesh sensitivity is performed according to the mesh resolution study in FDS Uses' guides (Kevin McGrattan *et al.* 2015) to choose the appropriate mesh grid. The calculation results is independent of the mesh density when there is no significant difference between different gird sizes. Then a comparison of the present numerical results and experimental data is presented. A small car fire of 4MW is discussed in the following section.

For simulation involving fire plumes, a non-dimensional expression$D^*/\delta x$ is given to calculate the grid size suitable for credible simulations, where D^* is a characteristic fire diameter

$$D^* = \left(\frac{\dot{Q}}{\rho_\infty c_P T_\infty \sqrt{g}}\right)^{\frac{2}{5}} \qquad (9)$$

and δx is the nominal size of a mesh cell (Kevin McGrattan *et al.* 2015). It is recommended by McGrattan that the value of $D^*/\delta x$ should be in the range of 4 to 16. Therefore, the grid size of the mesh

for a 4MW (heat release rate for a car) fire was calculated to be between 0.104m and 0.417m.

Five different grid sizes ranging from 0.1m to 0.4m are chosen for the sensitivity analysis in this paper, as shown in Table 1. The range of the computational domain will have an obvious influence on the temperature and velocity distribution in the tunnel because of the flow in and out of the tunnel. Therefore, an additional computational regions are added near the tunnel outlets, which is determined according to the parametric study of computational domain on numerical simulation by He *et al.* (1998).
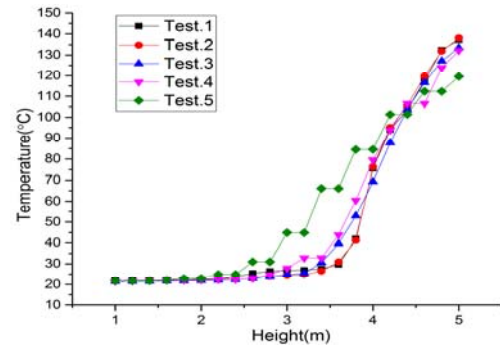

Fig. 1. The vertical temperature profiles 40m from the fire source.
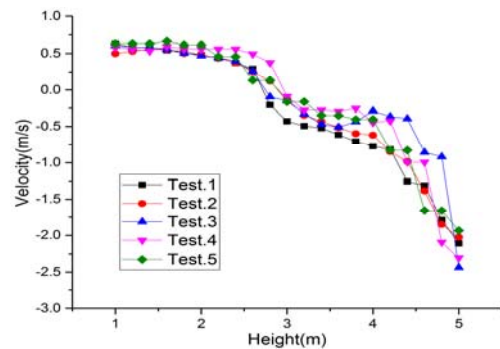

Fig. 2. The vertical velocity profiles 40m from the fire source.

Figure 1 and Fig. 2 presents the vertical temperature and velocity profiles in the tunnel with different mesh density. As shown in the figures, with the mesh density increasing, the temperature and velocity curves trend to be uniform. The simulation results of mesh with 0.15 m and 0.1 m get little difference, that is to say, when the mesh size is less than 0.15m, the simulation results did not improve significant, but it

takes more time. Hence, 0.15m grid system is adopted for researching smoke diffusion in tunnel in order to obtain accurate simulation results.

The flow characteristics of computational fluid dynamic model is validated by comparing the numerical prediction with the full scale experimental data. Considering the geometrical shape of the model and the fire source used in the experiments, the experiment data from Hu *et al.* (2006) are selected for validation. The relationship between numerical simulation and full scale experiments according to the Froude modelling (Yoon *et al.* 2006) is given by

$$\frac{Q_s}{Q_e} = \left(\frac{L_s}{L_e}\right)^{\frac{5}{2}} \tag{10}$$

$$T_s = T_e \tag{11}$$

Where Q is the heat release rate (HRR), T is the temperature (K), L is the physical model size. The subscript 's' represent full scale experiment, the subscript 'e' is for the numerical simulation.

A set of full scale tests were carried out in an underground corridor measuring 88m long, 8m wide and 2.65m high with heat release rate 0.8MW and 1.5MW by Hu *et al.* (2006), and we compared the maximum ceiling temperature and the vertical temperature of numerical simulation with the experimental data from Hu's tests. Using the Eq. (10), the heat release rate 4MW in the simulation model equals to the heat release rate 1.3MW in the full-scale experiments. The longitudinal ceiling temperature in the simulation model and full-scale experiments with heat release rate 1.5MW are compared in the Fig. 3. In Fig. 3. a), the longitudinal temperature in full-scale experiments are higher than the simulation tests because of the fire source, the decay of smoke temperature in the simulations are consistent with measured temperature. In Fig. 3. b), vertical temperature are compared to validate the temperature deviation in both upper zone and lower zone, and vertical temperature in simulations show great consistence with the experimental data. Therefore, the accuracy of the numerical simulation results in this paper can be ensured through the gird sensitivity and the comparison with experiments.

2.3 Physical Model Setup

Taking an actual tunnel as the prototype, the tunnel model in this paper is 100m long, 8.1m wide and 5.1m high. The ceiling is flat and the left and right ends of the tunnel are set to be "OPEN" with no initial velocity. The fire source is located in the longitudinal centreline of the tunnel, 30m away from the left end of the tunnel. The mechanical vent is 3m long and 1m wide, 4m high from the ground, which was mounted in the side wall and 30m away from the fire source. The schematic diagram of the physical model is shown in Fig. 4. By taking the several typical vehicles into account, the fire heat rates (HRRs) (PIARC Committee on Road Tunnels (C5) 1999) is designed as 4MW, 10MW, 20MW, 50MW and 100MW to simulate the most common fire scenarios in the road

tunnels, listed in Table 2.
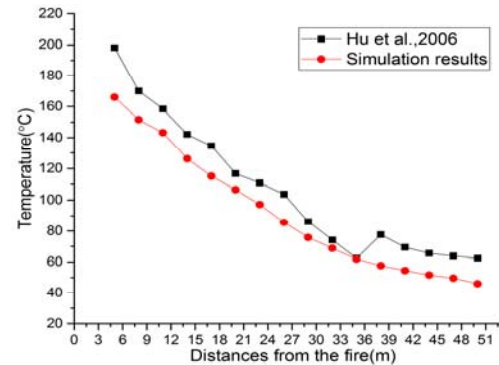
a) Longitudinal temperature comparison
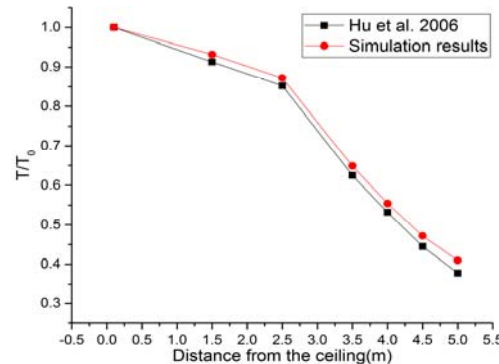
b) Vertical temperature comparison
Fig. 3. Comparisons with the experimental data.

Table 2 Heat release rate for different types of vehicles

Types of Vehicles	Heat Release Rate(MW)
Cars	4
Truck	10
Bus	20
Tank car	50
Large petrol tankers	100

According to <Guidelines for Design of Lighting of Highway Tunnels> (JTG/T D70/2-01-2014) 10.2.9, the velocity in the smoke vent should not greater than 10m/s, which means the exhaust rate of a single vent is under 30m³/s, so for each fire source, the exhaust rates with wide range are set from 2m³/s to 30m³/s, and the interval for the next simulation case is 2m³/s. In addition, the fire scenarios without smoke exhaust are also simulated as the controlled group. The ambient air temperature and the initial temperature of tunnel wall are set to be 20°C. The tunnel constructions are specified as "CONCRETE" and its density, specific heat and conductivity are 2280.2kg/m³, 1.04kJ/(kg*K), 1.8W/(m*K). The ambient pressure in the tunnel is 1.01E5 Pa, the ambient oxygen Mass Fraction is 0.232378 kg/kg. The relative humidity in the computational domain is about 40% (Kevin McGrattan *et al.* 2015).
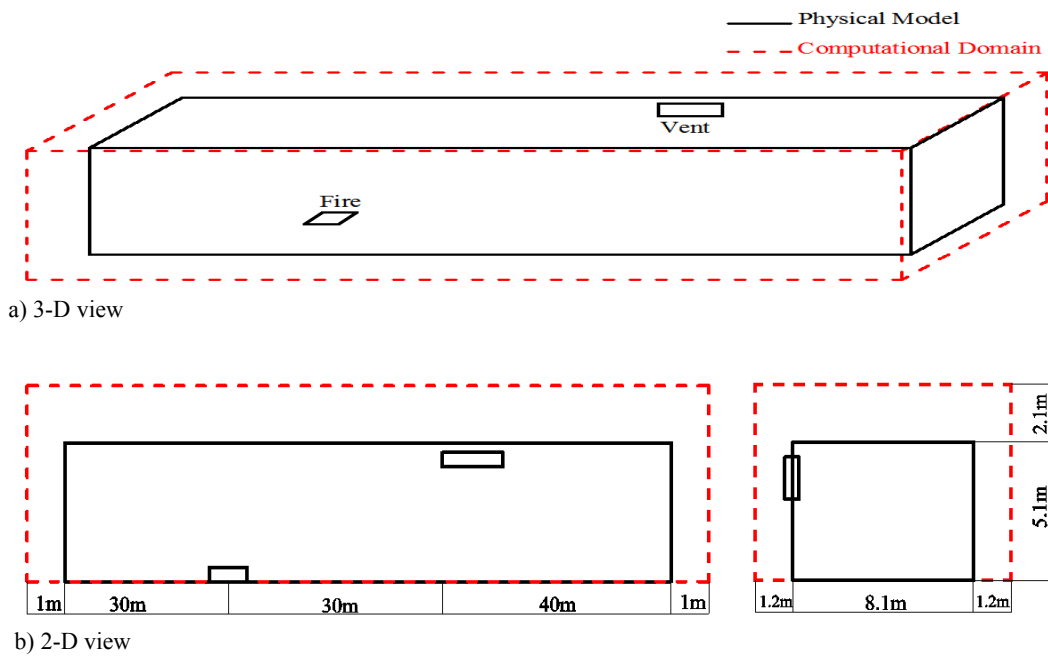
a) 3-D view

b) 2-D view

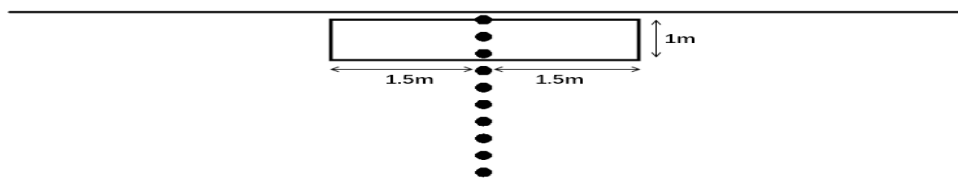**Fig. 4. The schematic diagram of the tunnel.**

Fig. 5. Positions of the thermocouples in the fire tests.

The arrangement of the measuring points is shown in Fig. 5. A column of 11 thermocouples and the layer device are located near the smoke vent to estimate the condition of smoke exhaust process. The thermocouples are set up with 0.2m spacing and the highest ones were 0.1m below the ceiling. The important properties of thermocouples used in this study are as follows: the value for bead diameter is 0.001m, the emissivity is 0.85. The values for the bead sentisy and specific heat are that of nickel; 8908 kg/m3 and 0.44 kJ/kg/K, respectively (Kevin McGrattan *et al.* 2015).

3.   RESULTS AND DISCUSSIONS

3.1   Smoke Characteristic Near the Lateral Smoke Vent

Figure 6 presents the temperature distributions in the tunnel near the smoke vent at different exhaust rates on the heat release rate 4MW. Fig. 6 a) is the controlled test, as shown in Fig. 6 a), the temperature in the lower part of tunnel is about 20-30°C. The hot smoke flows upward and occupies the upper area of the tunnel, the temperature of the upper area is over 100°C. A interface is located between the hot smoke and cold air in the tunnel without exhaust rate, and the stable smoke stratification exist when the exhaust rate is small enough and the buoyancy forces is strong enough. The interface in the Fig. 6 a) is below

the lower edge of the vent, the smoke vent is covered by the hot smoke layer.

For Comparing to the case of no smoke exhausting shown in Fig. 6 a), disturbance on smoke interface in Fig. 6 b)- d) is enhanced due to the smoke exhausting process. As shown in Fig. 6 b), the smoke exhaust rate is 2m3/s, the smoke layer becomes thinner and the smoke layer interface reached the lower edge of the smoke vent interface. In the Fig. 6 c) - d), with the exhaust rate increasing, more smoke is removed from the smoke vent and a sunken area appears in the middle of the smoke vent. In the Fig. 6 e) - f), more cold air is inhaled into the smoke vent with the exhaust rate increasing, leading to the sunken area below the smoke vent bigger and bigger, When the exhaust rate reaches a certain value, the sunken area maintains a certain area and the highest point of sunken area maintains.

The velocity vector graphs with different exhaust rate are listed in Fig. 7, Heat release rate of 4MW is taken as example again. As shown in Fig. 7 a), the velocity vector in the lower and upper part of the field is uniform and the flow tendency is contrary because of the buoyancy force. There exist some small-scale vortexes in the transition zone between the hot smoke layer and the cold air in Fig. 7 b) and the streamline of lower layer is basically horizontal, i.e., the mass flow rate exhausted through the lateral vent are mainly from the upper smoke layer. With the
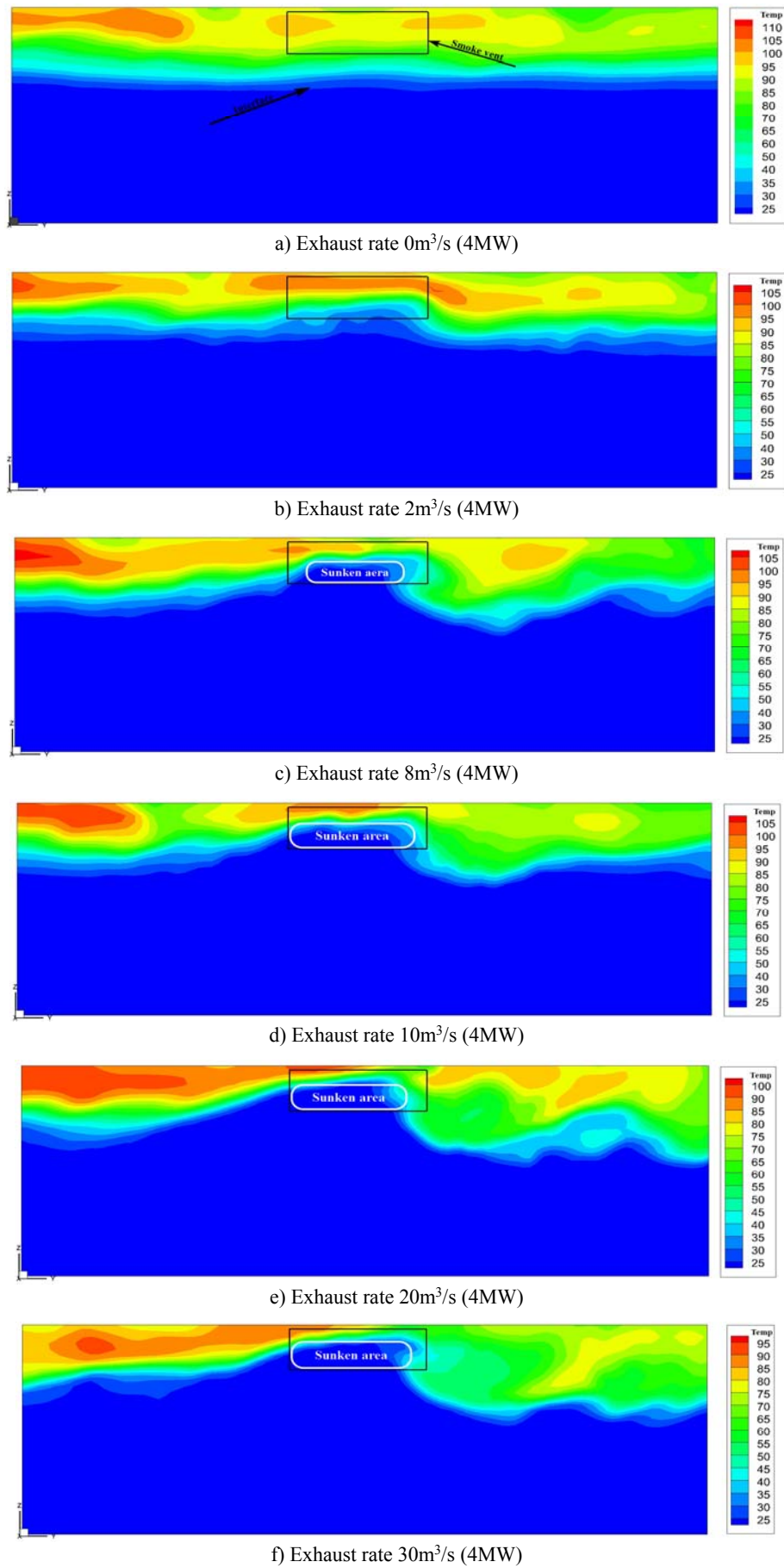
a) Exhaust rate 0m³/s (4MW)

b) Exhaust rate 2m³/s (4MW)

c) Exhaust rate 8m³/s (4MW)

d) Exhaust rate 10m³/s (4MW)

e) Exhaust rate 20m³/s (4MW)

f) Exhaust rate 30m³/s (4MW)

Fig. 6. The temperature distributions in the tunnel near the smoke vent at different exhaust rates.

a) Exhaust rate 0m³/s (4MW)

b) Exhaust rate 2m³/s (4MW)

c) Exhaust rate 8m³/s (4MW)

d) Exhaust rate 10m³/s (4MW)

e) Exhaust rate 20m³/s (4MW)
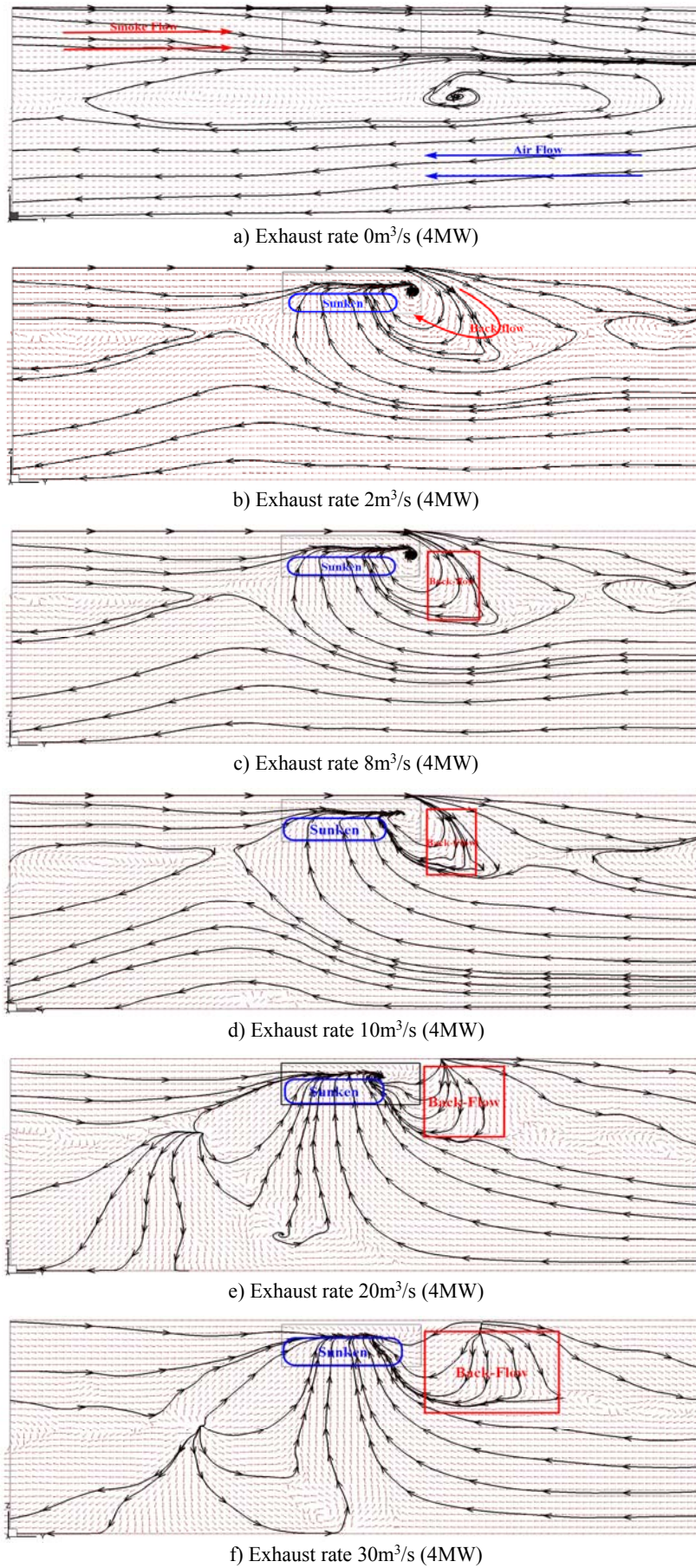
f) Exhaust rate 30m³/s (4MW)
Fig. 7. Velocity vector field in the tunnel.

a) No plug-holing

b) Plug-holing
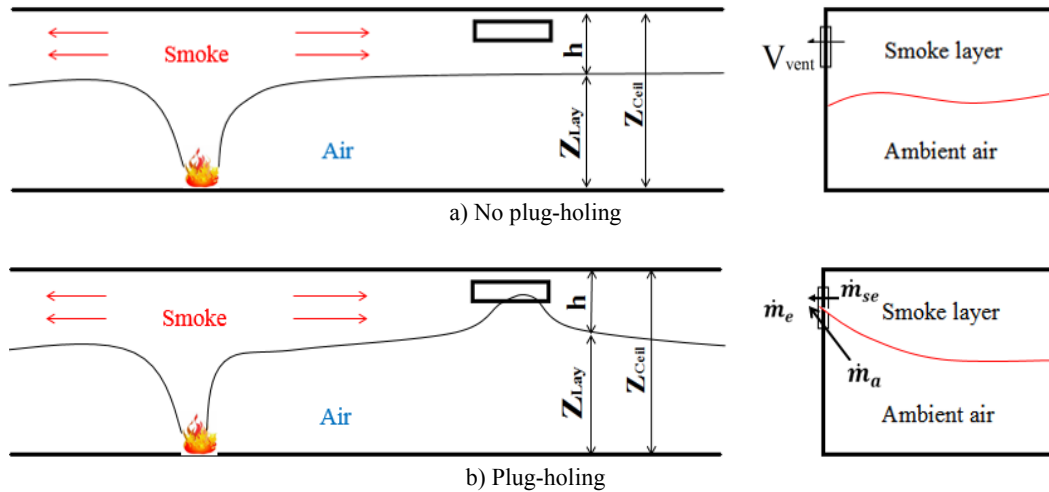**Fig. 8. The sketch of lateral exhaust progress.**

exhaust rate increasing, the height of smoke layer becomes higher and the sunken area becomes bigger, in Fig. 7 c)- f), the disturbance on smoke interface is enhanced due to the large exhaust rate, and the fresh air in the lower part of tunnel are sunken into the vent, while the downstream hot smoke layer is back-flow. When the exhaust rate reach 20m³/s, the lower streamline turns to upwards and more and more fresh air will be inhaled into the smoke vent, which could lead to a poor exhausting efficiency.

3.2 The Phenomenon of the Plug-Holing

The smoke extraction process with the smoke being extracted through a lateral vent is shown in Fig. 8. Referring to Fig. 8 a), this depicts the smoke being extracted through the lateral smoke vent when the plug-holing have not occurred, the smoke vent is covered by the hot smoke induced by fire, and in the Fig. 8 b). The fresh air is sucked into the smoke extraction system when the plug-holing have occurred.

Hinkley *et al.* (2002) investigated the plug-holing phenomenon in the natural smoke extraction system using an opening without a vertical shaft. A Froude number was proposed to predict the occurrence of plug-holing in his study. Some experiments were carried out in a small-scale atrium to study the plug-holing using a mechanical extraction system by Lougheed *et al.* (2002). He found that the Froude number proposed by Hinkley can also be adopted in the mechanical smoke extraction system. Vauquelin (2008) noticed that the phenomenon of plug-holing using a small-scale tunnel and concluded that the smoke extraction efficiency had decreased obviously due to the occurrence of plug-holing. Froude number is calculated in this paper by

$$Fr = \frac{V_{vent} * A_{vent}}{(g\Delta T/T_0)^{\frac{1}{2}} d^{\frac{5}{2}}} \qquad (12)$$

$$d = Z_{CEIL} - Z_{LAY} \qquad (13)$$

Where, F is the Froude number, V_{vent} is the flow velocity through smoke vent (m/s), A_{vent} is the area of the smoke vent (m²), g is the gravity acceleration

(m²/s), delta T is the average temperature rise of the smoke layer (K), T_0 is the ambient temperature (K), d is the depth of the smoke layer (m), Z_{ceil} is the height of the ceiling (m), Z_{lay} is the height of smoke layer (m) (Leonard Y. Cooper 2002).

A horizontal interface is located between the upper smoke layer generated in the fire plume and the lower cool air. In the former researches, some methods have been studied to calculate the interface height, for example, N-percentage rule by Cooper *et al.* (1982)., the upper zone averaging and mass equivalency technique by Quintiere *et al.* (1984) a combination of the method by Quintiere *et al.* and the maximum gradient method by Emmons *et al.* (1978) developed by Janssens and Tran (1992). N-percentage rule is one of these most widely used methods to determine the interface height given as:

$$T_{int} - T_{amb} = (T_{max} - T_{amb}) \times \frac{N}{100} \qquad (14)$$

Where, T_{int} is the temperature at the interface (K), T_{amb} is the temperature of ambient air (K), T_{max} is the maximum temperature of smoke layer (K). Different values (10, 15 and 20) have been suggested in the enclosure compartment by Cooper *et al.* (1982), and in the former literatures, Ji *et al.* (2013) have researched the optimum N value in a 1/6th reduced scale tunnel which could be admitted in tunnel fires, and found out that N=20 has the best agreement with the experimental data, which is adopted in this paper. The temperature of interface calculated by the N-percentage rule was given in the

Table 3 Temperature of smoke layer

Heat Release Rate (MW)	Tmax (°C)	Tint (°C)
4	95.5	35
10	148.6	45
20	226.1	62
50	340.6	84
100	468.8	110

Table 3 Temperature of smoke layer

Heat Release Rate (MW)	T_{max} (°C)	T_{int} (°C)
4	95.5	35
10	148.6	45
20	226.1	62
50	340.6	84
100	468.8	110

3.3 Exhausting Efficiency

As shown in Fig. 8 b), under a fire condition, a mixture of smoke and fresh air will be extracted into the mechanical exhaust system. The smoke exhaust rate of the lateral smoke vent, $\dot{m}_e$ can be classified into two parts:

$$\dot{m}_e = \dot{m}_{se} + \dot{m}_a \tag{15}$$

$$\text{VSO} = \frac{\dot{m}_{se}}{\dot{m}_e} \tag{16}$$

Where $\dot{m}_{se}$ is the smoke proportion in the exhaust rate and $\dot{m}_a$ is the amount of the fresh air. To achieve a better extraction efficiency, $\dot{m}_a$ should be exhausted as little as possible. The ventilation system output (VSO) is an important parameter in a transverse ventilation system. By definition, the VSO is calculated by the ratio of the extracted smoke flow rate to the extraction flow rate referring to Eq. (16). The VSO for all tests is shown in Fig. 9, as we can see from the Fig. 9, the VSO decreases with the exhaust rate increasing, that is to say, more fresh air are entrained into the exhaust vent. As the exhaust rate increase to the certain value, the VSO is less than 0.5, under this condition, more than half of the mixture drawn into the smoke vent is fresh air rather than smoke.
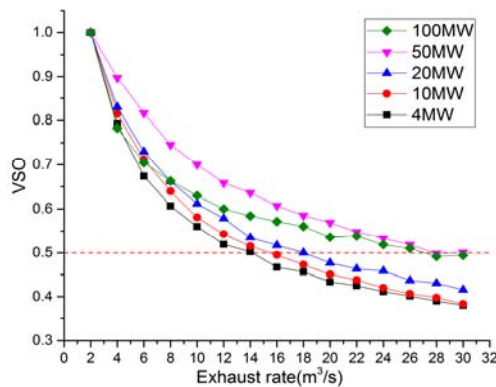

Fig. 9. The VSO calculated for all tests.

3.4 Calculation of Froude Number

Figure 10 represents the depth of smoke layer variation with exhaust rate on the different heat release rate. The depth of smoke layer is obtained by the Eq. (13). In FDS, the method of calculating the smoke layer height is proposed by Janssens et al. (1992). From Fig. 10, it can be seen that depth of smoke layer changes with the increase of exhaust rate. At first, the depth of smoke layer decreases

quickly with the increase of exhaust rate, when the smoke layer reaches to the lower edge of lateral smoke vent (critical point), the fresh air is sunken into smoke vent, i.e. the plug-holing occurs. When the smoke layer reaches to 0.5 meter (saturated point), the depth of smoke layer changes gentle, that is to say, increasing the exhaust rate does not exhaust out more smoke but fresh air, the exhausting process is saturated under this condition. In the former researches, there is a critical Froude number named as $Fr_{critical}$ for the occurrence of the plug-holing, in this paper, the critical Froude number happen when the depth of smoke layer reach to lower ledge of the smoke vent (1.1m). And, a saturated Froude Number $Fr_{saturated}$ was adopted in this paper to represent that when the Froude number calculated under the certain exhaust rate is greater than $Fr_{saturated}$, the exhaust efficiency will not increase with the increase of exhaust rate.
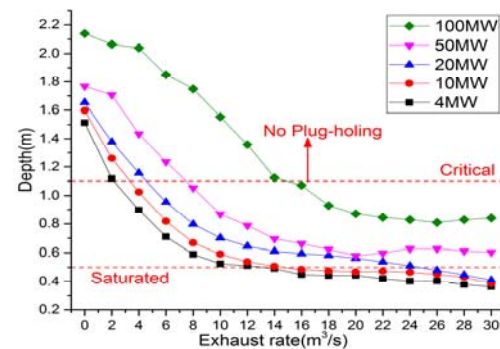

Fig. 10. Depth of smoke layer.

Figure 11 represents the temperature profiles measured by the thermocouple tree near the lateral smoke vent. As shown in Fig. 11, under a certain heat release rate (HRR) and a certain exhaust rate, the maximum temperature appear at the tunnel ceiling due to the thermal buoyancy effect. The temperature decrease with the height of thermocouple decreasing. Under a certain heat release rate (HRR) and a certain height, the temperature decreases with of the exhaust rate increasing and then changes gently after a certain exhaust rate. When the exhaust rate is small enough, smoke is removed from smoke vent and the smoke layer interface is still below the lower edge of the smoke vent. Then fresh air below the smoke layer is inhaled into the smoke vent due to the increasing exhaust rate, and the Froude number under this exhaust rate is the critical Froude number. As the exhaust rate increasing, the thickness of the smoke layer becomes thinner. When the exhaust rate increase to a certain value, the thickness of smoke layer changes gentle, and the Froude number under this exhaust rate is proposed as the saturated Froude number.

As the hot gases spread to the upstream and downstream of the fire source, the temperature beneath the tunnel ceiling is higher than the lower smoke layer. It can be seen in the Fig. 11 that temperature at the height of 5.0m and 4.8m are the maximum temperature at the same heat release rate and exhaust rate and does not change significant with the increasing of exhaust rate. More smoke is removed

from the smoke vent and the depth of smoke layer decreases with the increasing of exhaust rate.

It can be seen from the isothermal curves, when the smoke layer interface is higher than the low edge of the vent, the phenomenon of plug-holing occurs, the

Froude number calculated under this exhaust rate is $Fr_{critical}$. Then when the depth of smoke layer does not change significant with the increasing of exhaust rate, the Froude number under this exhaust rate is the $Fr_{saturated}$. According to the critical exhaust rate

Table 4 Froude Number and the VSO

	4 MW	10 MW	20 MW	50 MW	100 MW	Average
$Fr_{critical}$	0.45	0.45	0.43	0.52	0.54	0.48
$Fr_{saturated}$	2.0	1.94	1.95	1.91	——	1.95
VSO	0.58	0.53	0.50	0.52	——	——

a) HRR=4MW

b) HRR=10MW

c) HRR=20MW
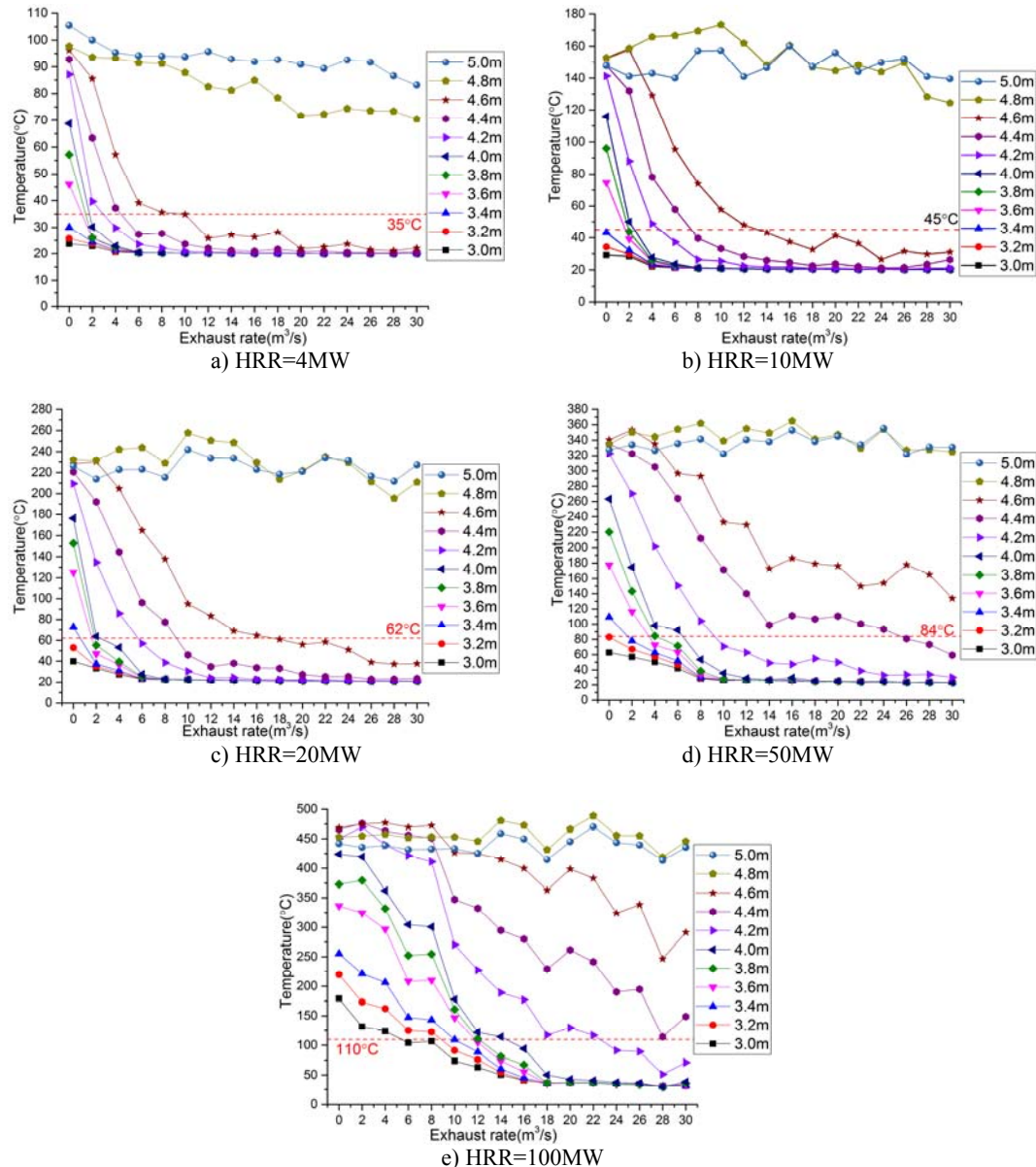

d) HRR=50MW

e) HRR=100MW

Fig. 11. Temperature measured near the vent from Z=3.0m to Z=5.0m.

determined by N-percent rule, we calculate the Froude number on each heat release rate by Eq. (12), as shown in Table 4, the critical and saturated Froude number on different fire power is 0.48 and 1.95 respectively. The VSO under the saturated Froude

number is also shown in Table.4, and these VSO is a little great than 0.5, that is to say, under the saturated condition, more than a half part of the smoke exhaust rate is smoke.

Figure 12 presents the Froude number on different heat release rate with different exhaust rate. According to our research, the critical Froude number is about 0.48 to determine the occurrence of the plug-holing in lateral smoke system, and a saturated Froude number about 1.95 is proposed for the engineering application. When the calculated Froude number is less than the critical Froude number 0.48, the extraction system remove the smoke induced by fire flume, no fresh air from the lower part have been drawn into the smoke vent. When the calculated Froude number is greater than the saturated Froude number 1.95, more than a half of the extraction volume is fresh air rather than smoke, the efficiency of lateral extraction system decreases obviously.
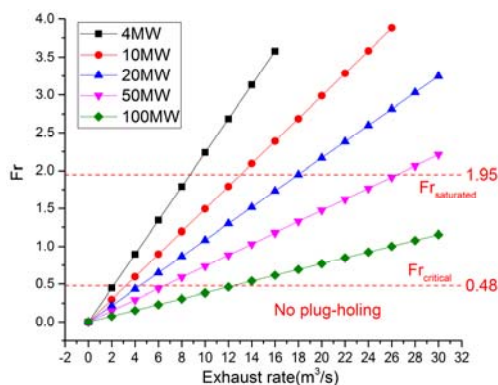

Fig. 12. Froude number on different heat release rate with different exhaust rate.

4. CONCLUSION

In this study, a set of numerical simulations were performed by using a FDS model tunnel to investigate the smoke flow characterization and the Froude number which determine the occurrence of the phenomenon of plug-holing under lateral smoke extraction system in the tunnel fire. In general, the occurrence of plug-holing under lateral smoke extraction system has a great relationship with the depth of smoke layer and the exhaust rate at the smoke vent, an appropriate exhaust rate should be adopted to obtain a better smoke efficiency and keep a good smoke stratification. Five different fire heat release rate of 4MW, 10MW, 20MW, 50MW, 100MW and the different extraction rates varying from 0m³/s to 30m³/s are considered. For tunnel with lateral smoke vent, smoke at the upstream of the vent can maintain a good stratification while the smoke stratification at the downstream dissolves due to the exhaust system. Results show that the phenomenon of plug-holing will influence the lateral smoke exhaust system performance. More cold air is inhaled into the smoke vent with the exhaust rate increasing, which leading to the sunken area bigger and bigger. The exhausting efficiency would not change significantly as the exhaust rate increasing. When the smoke layer interface is higher than the low edge of the vent, the phenomenon of plug-holing occurs, the Froude number calculated under this exhaust rate is $Fr_{critical}$. Then when the depth of

smoke layer does not change significant with the increasing of exhaust rate, the Froude number under this exhaust rate is the $Fr_{saturated}$. The critical Froude number we calculated to determine the phenomenon of plug-holing under lateral smoke exhaust in tunnel fire is 0.48, however, a saturated Froude number 1.95 was introduced according to the smoke layer depth which changing gentle while the exhaust rate reaches to a certain value.

The Froude number we calculated in this paper can be used for the design of lateral smoke extraction system in tunnel and subway, the saturated Froude number can be used to determine the appropriate exhaust rate, which can lead to a better extraction efficiency. Future work will focus on the determination of plug-holing phenomenon in the multiple points lateral smoke extraction system. A lot of experiments will be carried out to verify the applicability of the Froude number and investigate the air entrainment process in the multiple-points extraction system.

REFERENCES

Carvel Ricky. (2015). Review: A review of tunnel fire research from Edinburgh. *Fire Safety Journal.*

Chow, W. K. and J. Li (2015). Case study: Vehicle fire in a cross-harbour tunnel in Hong Kong. *Tunnelling and Underground Space Technology Incorporating Trenchless Technology Research* 16(1):23-30.

Ciambelli, P., M. G. Meo, P. Russo and S. Vaccaro (2011). Thermal Radiation Modelling in Tunnel Fires. *ADVANCES IN APPLIED MATHEMATICS AND MECHANICS*, 3(3), 327-353.

Cooper, L. Y., M. Harkleroad, J. Quintiere and W. Reinkinen (1982). An experimental study of upper hot layer stratification in full-scale multi-room fire scenarios. *Journal of Heat Transfer* 741-749.

Emmons, H. W., H. E. Miltler and L. N. Trefethen (1978). Computer Fire Code III. Harvard University Division of Applied Sciences, Home Fire Project Technical Report 25.

Gehandler, J., L. Eymann and M. Regeffe (2015). Limit-Based Fire Hazard Model for Evaluating Tunnel Life Safety. *Fire Technology* 51(3), 585-614.

Guo, C. and P. Hai Dong (2007). Research on the Emergency Rescue of Fire in Super-long

Railway Tunnel. *China Safety Science Journal*, 17(9), 153-158.

He, Y., A. Fernando and M. Luo (1998). Determination of interface height from measured parameter profile in enclosure fire experiment. *Fire Safety Journal*.

HP, M. and J. P. Gardner. (1990). Design principles for smoke ventilation in enclosed shopping centers. Br 186 Garston, UK: Building Research Establishment.

Hu, L. H., Y. Z. Li, R. Huo, L. Yi and W. K. Chow (2006). Full-scale experimental studies on mechanical smoke exhaust efficiency in an underground corridor. *Building and Environment* 41, 1622-1630.

Janssens, M. and H. C. Tran (1992). Data reduction of room tests for zone model validation. *Journal of Fire Science* 10(6), 528–555.

Lee, M. and N. HUR (2012). A DETAILED CFD SIMULATION OF THE 2003 DAEGU METRO STATION FIRE. *International Journal of Air-Conditioning and Refrigeration* 20, 1-11.

Leonard, Y. C. (2002). Smoke and Heat Venting, in Handbook of Fire Protection Engineering. Third Edition, Society of Fire Protection Engineers and National Fire Protection Association, Boston, MA, USA 228-230.

Li, L., Z. Gao, J. Ji, J. Han and J. Sun (2013). Research on the Phenomenon of Plug-holing under Mechanical Smoke Exhaust in Tunnel Fire. *Procedia Engineering* 62, 1112-1120.

Lougheed, G. D. and G. V. Hadjisophocleous (2001). Smoke hazards from fires in high places. *ASHRAE Journal* 43, 34.

Lougheed, G. D., G. V. Hadjisophocleous, C. J. Mccartney and B. C. Taber (2002). Large-scale physical model studies for an atrium smoke exhaust system. *ASHRAE Transactions*.

McGrattan, K., R. McDermott, C. Weinschenk and *et al*. (2015). NIST Special Publication 1019. Six Edition. National Institute of Standards Technology. *Fire Dynamics Simulator User's Guide*.

Quintiere, J. Q., K. Steckler and D. Corley. (1984). An assessment of fire induced flows in compartments. *Fire Science and Technology* 4, 1-14.

Richard, G. G. (2004). Sublethal Effects of Fire Smoke. *Fire Technology* 95-99.

Spratt, D. and A. J. M. Heselden (1974). Efficient extraction of smoke from a thin layer under a ceiling. *FIRE RESEARCH STATION*.

Tilley, N., P. Rauwoens and B. Merci (2011). Verification of the accuracy of CFD simulations in small-scale tunnel and atrium fire configurations. *Fire Safety Journal* 46, 186-193.

Vauquelin, O. (2008). Experimental simulations of fire-induced smoke control in tunnels using an "air–helium reduced scale model": Principle, limitations, results and future. *Tunnelling and Underground Space Technology* 23, 171-178.

Viot, J., O.Vauquelin and N. Rhodes (2001). Characterization of the Plug-holing Phenomenon for the Exhausting of a Low Density Gas Layer. *14th Australasian Fluid Mechanics Conference.* Adelaide University, Adelaide, Australia.

Vuilleumier, F., A. Weatherill and B. Crausaz (2002). Safety aspects of railway and road tunnel: example of the Lotschberg railway tunnel and Mont-Blanc road tunnel. *Tunnelling and Underground Space Technology* 17, 153-158.

Wen, J.X., Kang, K., Donchev, T., and Karwatzki, J.M. (2007). Validation of FDS for the prediction of medium-scale pool fires. *Fire Safety Journal*, 42, 127-138.

Yoon, C., Kim, M., and Kim, J. (2006). The evaluation of natural ventilation pressure in Korean long road tunnels with vertical shafts. *Tunnelling and Underground Space Technology*, 21, 472.